

Received November 26, 2020, accepted December 6, 2020, date of publication December 15, 2020,
date of current version December 31, 2020.

Digital Object Identifier 10.1109/ACCESS.2020.3044922

Minimization of Cogging Torque in Axial Field Flux Switching Machine Using Arc Shaped Triangular Magnets

MIRZA AAKIF BAIG¹, JUNAID IKRAM¹, ADNAN IFTIKHAR¹, (Member, IEEE),
SYED SABIR HUSSAIN BUKHARI^{1,2,3}, (Member, IEEE),
NASRULLAH KHAN¹, (Senior Member, IEEE),
AND JONG-SUK RO³

¹Department of Electrical and Computer Engineering, COMSATS University Islamabad, Islamabad 45550, Pakistan

²Department of Electrical Engineering, Sukkur IBA University, Sukkur 65200, Pakistan

³School of Electrical and Electronics Engineering, Chung-Ang University, Seoul 06974, South Korea

Corresponding author: Jong-Suk Ro (jongsukro@gmail.com)

This work was supported in part by the Basic Science Research Program through the National Research Foundation of Korea funded by the Ministry of Education under Grant 2016R1D1A1B01008058, in part by the Human Resources Development of the Korea Institute of Energy Technology Evaluation and Planning (KETEP) grant funded by the Korean Government Ministry of Trade, Industry and Energy, under Grant 20204030200090, and in part by the Korea Research Fellowship Program through the National Research Foundation (NRF) of Korea funded by the Ministry of Science and ICT under Grant 2019H1D3A1A01102988.

ABSTRACT Axial flux permanent magnet machine (AFPMM) provides high torque characteristics at low speeds without any mechanical gears. AFPMMs have numerous applications in wind energy, electric cars, and direct drive elevator applications. These machines have low cost and improved power to weight ratio. However, single sided AFPM suffers from torque ripples because of its non-sinusoidal back emf, cogging torque, and rotor eccentricity. There are two major components of pulsating torque, namely torque ripples and cogging torque. In PM machine design, the cogging torque is a serious concern because it adds unwanted harmonics to the pulsating torque. Whereas the torque ripples cause noise and vibrations. In order to gain high efficiency, torque ripples should be minimum. The aim of this research is to design “Slotted axial field flux switching permanent magnet machine”. Mathematical models are used to design the machine and Finite element method (FEM) has been used to analyze the machine. In addition, Latin hypercube sampling (LHS) has been used to create the samples. Finally, Kriging Method is used for approximating the model and genetic algorithm has been applied to get the optimum machine. The results showed 61.8 % reduction of the cogging torque in the proposed machine model as compared to the conventional one. Moreover, the optimized model further provided 6.15 % reduction in the cogging torque as compared to the proposed one.

INDEX TERMS Axial flux permanent magnet machine, cogging torque, slotted stator, flux switching, finite element method.

I. INTRODUCTION

Over the years, the permanent magnet (PM) machines are broadly used in power system in different types [1]–[5]. Amongst existing PM machines, Axial field PM machines show best performance due to its promising characteristics such as small axial length, small size, and high-power density [3]–[5]. Nonetheless, the traditional PM machine offers irreversible magnet demagnetization due to rise in rotor

The associate editor coordinating the review of this manuscript and approving it for publication was Christopher H. T. Lee¹.

temperature. On the other hand, Flux switching permanent magnet machine (FSPMM) has the ability to refrain from the irreversible demagnetization as both magnets and armature windings are placed in stator instead of the rotor [6]–[11]. The FSPMM has gained attraction in recent years because it has combined benefits of both PM synchronous machines and switching reluctance machines. Moreover, it has many desirable properties like increased torque/power density, robust structure, and excellent fault tolerance capabilities [12]. Fault tolerance capability is highly important in applications like aerospace and vehicle drive systems [13]–[14]. The idea of

FSPMM was first proposed in 1950's [15]. After that large number of FSPMM have been designed [16]–[20], which include 3-phase, multi-phase, E-core, C-core, axial, linear, and hybrid. Most of the designed FSPMM can attain high torque and power density but also suffer from high cogging torque and torque ripple due to its double salient structure and flux focusing effects. Therefore, it was necessary to reduce such torque pulsations in high performance applications to refrain from vibration and noise along with the provision of precise position and speed control [21]. In [22], a new alternate poles design was proposed. This machine offered high torque but had asymmetry in waveform of back EMF which may cause high torque ripples. In [12], Ackim Zlu studied flux switching machine with segmental rotor and PM primary excitation in segmental rotor. The rated voltage and rated torque were increased with the proposed model in [12], but at the cost of notable torque ripple. The main reason for increase in torque ripple was cogging torque, caused by deep tooting and slotting in stator.

Furthermore, W. Min and J. T Chen [17], proposed E-core and C-core linear switched flux PMM and compared it with the conventional linear SFPM machine. The proposed machine had small usage of magnet volume, whereas the C-core linear SFPM machine had the highest back EMF and force density due to increase in slot area. Contrarily, the proposed E-core machine had isolated coils, which were feasible for fault tolerance, but the peak-to-peak value of the cogging force was on a higher side as compared to the conventional machine. Similarly, Xiaohong Xue [16], designed a five-phase modular FSPMM with 18 and 19 rotor poles. The electromagnetic characteristics such as flux, back EMF, cogging torque, and unbalanced magnetic force (UMF) were studied. The results showed that the proposed machine not only retained the benefits of the conventional machines, but also offered less cost and enhanced fault tolerant capabilities. Also, the machine having 19 rotor poles incorporated the benefits of symmetric back EMF and decreased cogging torque but suffered from UMF. In [20], a hybrid excited FSPMM was proposed with the addition of iron flux bridges. A simple lumped parameter magnetic circuit model (LPMCM) was established which predicted the effects of different parameters. The study revealed that the field coil excitation (FEC) was increased by adding iron flux bridges, however the torque density was decreased. Li Hao proposed a novel dual rotor axial field FSPMM [23]. The study included the effect of the rotor pole width and stator chamfer slot on the back EMF and the cogging torque. There was an improvement in the waveform of the back EMF and reduction in the cogging torque by altering the rotor pole width to 1.4 ~ 1.6 times as compared to the conventional design and chamfering the stator slot. However, the output torque was significantly reduced. In [21], the torque characteristics of the FSPMM with rotor step skewing were studied. Two models with 10 and 14 rotor pole numbers were proposed. The rotor step skewing technique was adopted to decrease the cogging torque and the torque ripple, but the output torque obtained

was not desirable. Li Hao in [24], proposed a novel axial field FSPMM with U-shaped stator segments. The flux linkage and the back EMF of the proposed machine was mainly sinusoidal, but a very low output power of 0.6 kW. Wenliang Zhao [25], proposed a novel dual rotor axial field fault tolerant FSPMM. The proposed machine incorporated the benefits of phase group concentrated coil (PGCC) winding, and unaligned arrangement of both rotors. The PGCC winding was adopted to gain unity winding factor. The effects of flux focusing were increased by using spoke type permanent magnets. The cogging torque and torque ripple were reduced by using unaligned arrangement of both the rotors. Besides,, different techniques such as rotor side modification had been adopted for minimizing cogging torque and torque ripples. The rotor side modification techniques include magnet skewing and magnet displacement. But these techniques decreased the cogging torque at the cost of either asymmetry in the waveform of the back EMF or significant decrease in the rated power of the machine. The cogging torque is one of the main constraints in the FSPMM as magnets are placed in stator of FSPMM. Therefore, it is imperative to reduce cogging torque in FSPMM.

In this article, an axial field FSPMM with an arc shaped triangular magnets is presented. The proposed model has merits of low cogging torque due to greater effective air gap length. A detailed comparison has been done between the conventional and the proposed FSPMM, under same design parameters, using 3-D Finite Element Method (FEM). Furthermore, the proposed model is optimized using PM overhang configuration. The optimized model is obtained using GA followed by the approximation of model using Kriging method. The rest of the article is organized as follows: Section II discuss the governing numerical equations of the machine design, whereas comparison between the proposed and conventional FSPMM is explored in Section III. Model optimization is briefly discussed in Section IV followed by the conclusion of this research in Section V.

II. MACHINE DESIGN

In this section, basic numerical equations that are used for the machine design are briefly discussed to mathematically demonstrate the machine parameters responsible for output current and torque. The back EMF of the FSPMM must be sinusoidal [15]. Ignoring voltage drop in the stator resistance, input power P_{in} can be represented mathematically as:

$$P_{in} = 2 \frac{m}{T} \int_0^T E_m \sin(\omega t) I_m \sin(\omega t) dt, \quad (1)$$

where m , E_m , and I_m denote phase number, amplitude of back EMF, and current, respectively. The output power P_{out} is calculated using:

$$P_{out} = \gamma m E_m I_m, \quad (2)$$

where γ denotes efficiency. The flux in the machine is computed using:

$$\varphi = \varphi_m \cos(N_p \alpha_r), \quad (3)$$

where φ_m is magnitude of flux, N_p and α_r denotes the rotor pole number and rotor position, respectively. Further, the back EMF is expressed as:

$$e(t) = N_{ph}\omega_r N_p \varphi_m \sin(N_p \alpha_r) \quad (4)$$

In (4), N_{ph} and ω_r represents phase coil turns and angular speed of rotor, respectively. Ignoring the sinusoidal term in (4) and substituting value of φ_m from (3), we get:

$$e(t) = N_{ph}\omega_r N_p k_d k_f B_g \alpha_i \frac{1}{N_s} \frac{\pi}{4} (D_{out}^2 - D_{in}^2) \quad (5)$$

Eq. (5) shows that B_g is the peak value of the air gap flux density, k_d is coefficient of the leakage flux, k_f is the coefficient of the air gap flux density distribution, α_i is pole arc coefficient, and N_s is the number of slots. D_{out} and D_{in} are outer and inner diameter of the rotor and the stator, respectively.

The armature current of the machine is determined by:

$$I_m = \frac{\sqrt{2} A_e \pi D_{in}}{2m N_{ph}}, \quad (6)$$

where A_e is electrical loading.

The mathematical relation of the cogging torque and air gap flux density is:

$$T_{cogg} = -\frac{1}{2} \phi_g^2 \frac{dR}{d\theta} \quad (7)$$

ϕ_g is the air gap flux, R is the reluctance of the air gap, and θ is the rotor position.

Substituting (5), (6), and $\omega_r = \frac{2\pi n_{rpm}}{60}$ in (2) give rise to:

$$P_{in} = \frac{\sqrt{2\pi^3}}{240} \frac{N_p}{N_s} k_d k_f k_{io} (1 - k_{io}^2) A_e B_g \alpha_i D_{out}^3 n_{rpm} \gamma \quad (8)$$

In (8), k_{io} is ratio of inner diameter to outer diameter and n_{rpm} is the rotor speed in rpm. Whereas the output torque is given by:

$$T_{out} = \frac{\sqrt{2}}{8} \pi^2 \frac{N_p}{N_s} k_d k_f k_{io} (1 - k_{io}^2) A_e B_g \alpha_i D_{out}^3 \gamma \quad (9)$$

It is obvious from (8) and (9), that the output power and torque are directly related to N_p/N_s , B_g , and A_e .

From (7), the outer diameter is given as:

$$D_{out} = \sqrt[3]{\frac{240 P_{out} N_s}{\sqrt{2} \pi^3 N_r k_d k_f k_{io} (1 - k_{io}^2) A_e B_g \alpha_i n_{rpm} \gamma}} \quad (10)$$

III. COMPARISON BETWEEN CONVENTIONAL AND PROPOSED MODEL

This section presents a detailed geometrical difference between the conventional and the proposed models. The machine model consisting of rectangular shaped magnet is named as ‘conventional shape’ while an arc shaped triangular magnet used in the machine model is named as ‘proposed shape’.

A. ARC SHAPED TRIANGULAR MAGNETS (THE PROPOSED SHAPE)

Figure 1 shows geometry of the rectangular shaped magnets used in the machine and the proposed ‘arc shaped triangular magnets’. W_o and H_o shown in Figure 1 represent PM width and PM height, respectively.

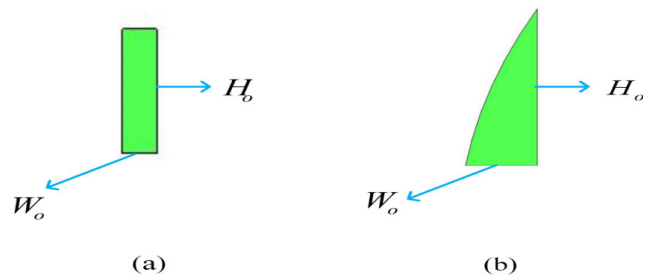


FIGURE 1. Geometry of the magnet (a) The conventional magnet and (b) the proposed arc shaped magnet.

B. PERFORMANCE COMPARISON BETWEEN CONVENTIONAL AND PROPOSED MODEL

The topologies of the designed FSPMMs are shown in Figure 2. Both machines have 12 stator slots and 13 rotor poles. The outer/inner diameter, axial length, stator tooth width, air gap length, phase coil turns, and magnet volume are kept same for both the models. Figure 2 (a) shows a complete design of the FSPMM with rectangular magnets i.e., the conventional one. Whereas it can be observed from Figure 2 (b) that topology of the designed FSPMM is same except the novel shape of the magnets which is arc shaped (the proposed one). For the rest of discussion in the article, Axial field FSPMM with rectangular magnets is named as ‘the conventional model’ while axial field FSPMM with arc shaped triangular magnets is referred as ‘the proposed model’. Due to low cost, ferrite magnets with circumferential magnetized direction and opposite polarity alternatively are inserted in stator. The rotor and stator core are made up of 50NSSMC 470. The design parameters of both the models are shown in Table 1. The topologies shown in Figure 2 are designed in JMEG software and same design parameters are used for both the designs. The results of the both the models are computed using FEM analysis in JMEG software. The flux density distribution of the conventional and the proposed models shown in Figure 3. It can be seen in Figure 3 that maximum magnetic flux density B_{max} is 1.8 T. B_{max} is usually considered for examining the saturation in rotor back iron. It can also be observed from Figure 3 that total magnetic flux density is comparatively less in the proposed model as compared to the conventional model. This is attributed to increased air gap length because of the arc shaped magnets in the proposed model.

Next, the back emf computation results of both the models shown in Figure 4 reveal that there is 3.0 V reduction in the proposed model than the conventional machine. The proposed arc shaped magnets in fact reduce the magnetic flux which is directly related to the voltage. However,

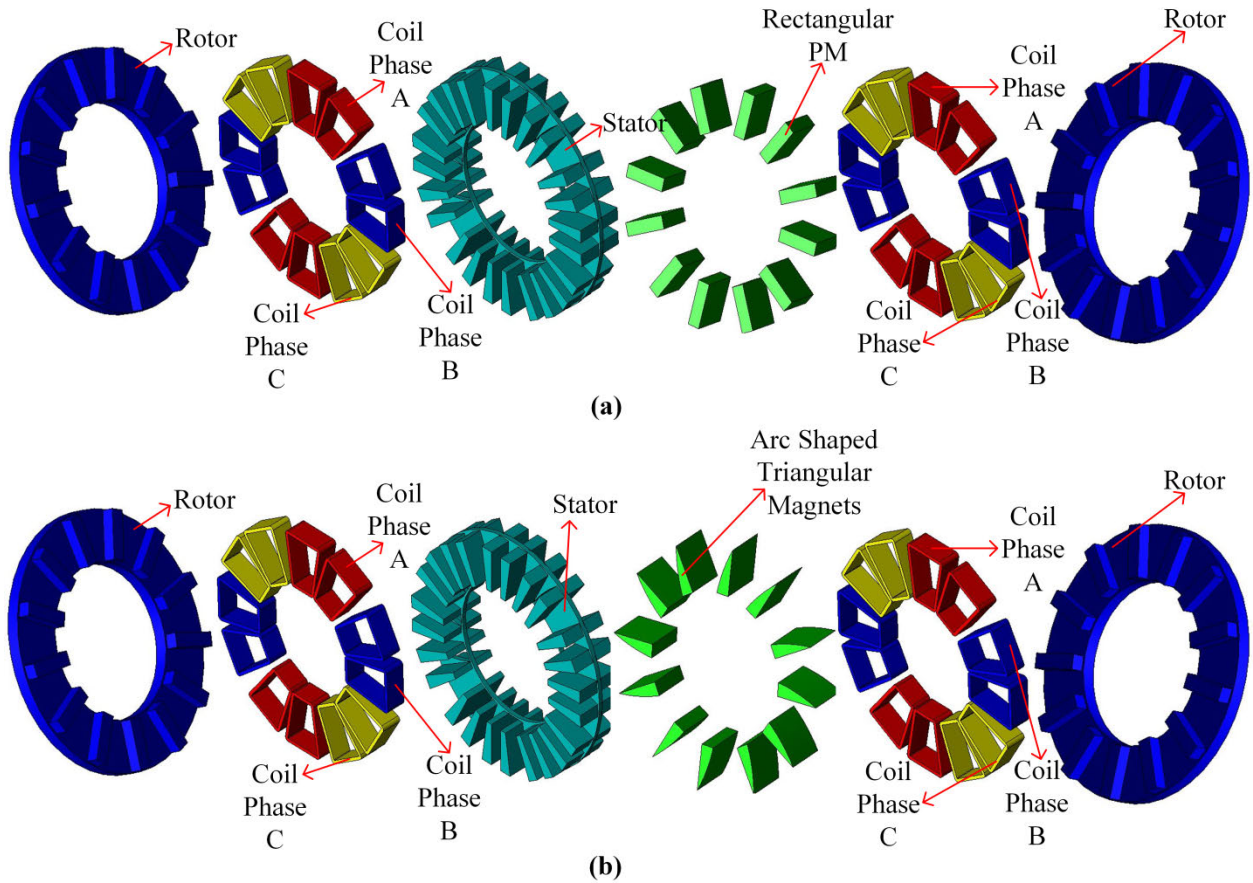


FIGURE 2. The adopted topologies of the FSPMM (a) The conventional model and (b) the proposed model.

TABLE 1. Design Parameters of Conventional and Proposed Models

Parameters	Conventional model	Proposed model	Parameters	Conventional model	Proposed model
Magnet	12 on both		Speed	450 rpm	
Coils	24 on both		Coil height	24mm	
Area of Magnets	655mm ²	389.5mm ²	Axial length	106mm	108mm
Stator yoke depth	5mm		Air gap length	1.2mm	
Stator Tooth height	54.8mm		Coil resistance	0.015 ohm	
Rotor yoke depth	12.5mm		Total Magnet thickness	10mm	
Area of coil	781mm ²		Phase Coil Turns	192	
Magnet	Ferrite		Core	50H470	

the total harmonic distortion (THD) is improved in proposed model. The THD is 2.2% and 1.7% in conventional and proposed models, respectively. The reason for reduction in THD is that more sinusoidal waveform of flux density distribution is achieved with the proposed arc shaped triangular magnet.

Finally, Figure 5 shows the comparison of the cogging torque of both the models. It is obvious from Figure 5 that

the cogging torque is greatly reduced in the proposed model. Overall, there is 61.8% reduction in peak-to-peak value of the cogging torque as compared to conventional model. The insertion of the arc shaped magnets decreases total magnetic flux density by increasing effective air gap length as compared to the conventional rectangular shaped magnets. This effective length reduction in the air gap significantly decreases the flux between permanent

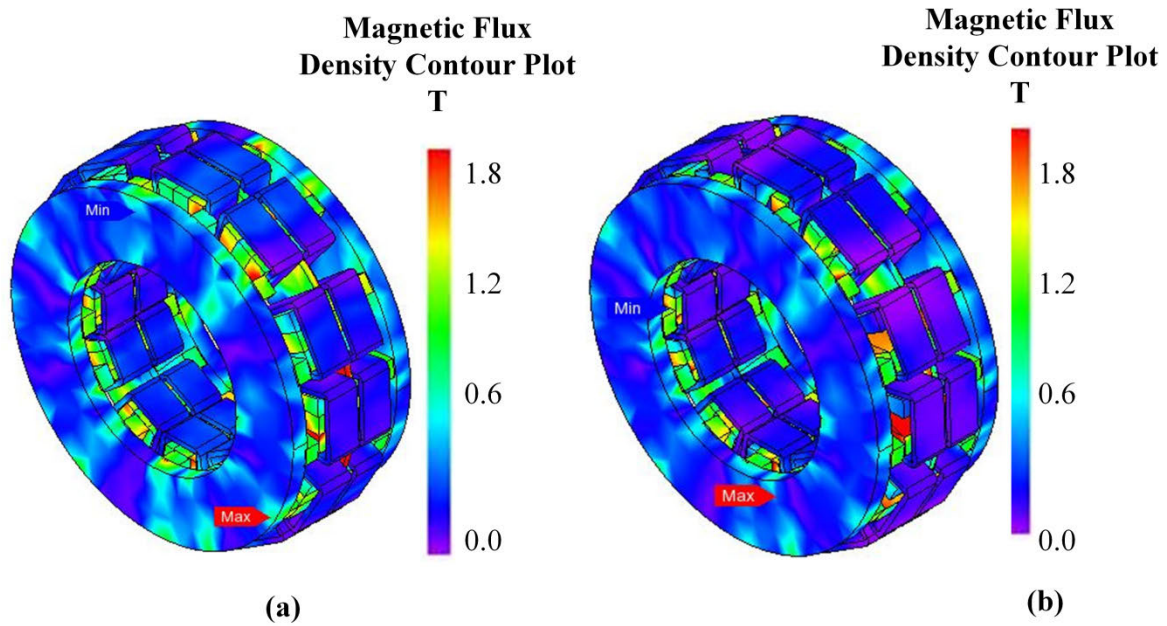


FIGURE 3. Flux density distribution (a) conventional model, and (b) proposed model.

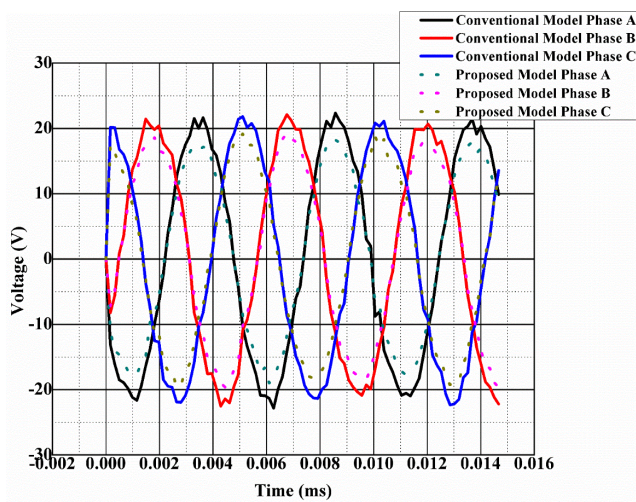


FIGURE 4. Back EMF comparison of the conventional and the proposed models.

magnets which as a result, reduce the cogging torque. On the contrary, reduction in the rated torque is observed in the proposed model. The rated torque of the conventional and the proposed models is 61 Nm and 57.2 Nm, respectively.

IV. OPTIMIZATION

To further enhance the performance of the proposed model, optimization is performed while keeping the magnets' volume constant

A. DESIGN VARIABLES

The concept of magnet overhang is used in optimization. The length of PM is varied along outer and inner radii. More

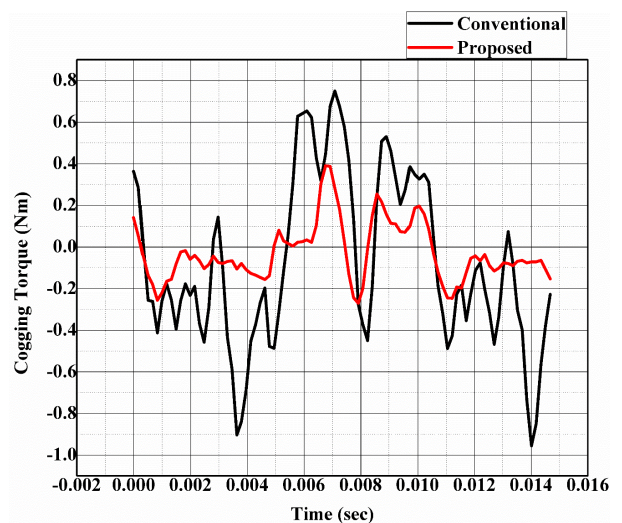


FIGURE 5. Cogging torque comparison between the conventional and the proposed models.

specifically, the length of the PM is varied from outer radius of the disc, known as upper overhang and the length of the PM is varied from inner radius of the disc, known as lower overhang. The arc of the PM is also varied. The variation of the arc results in reduction of the cogging torque. The design variables X_1 and X_2 are the overhang length and an arc of PM, respectively, as shown in Figure 6. The volume of the PM is kept equal by altering the height (H_o). The variables R_{arc} , θ_{arc} , and H_o denote the radius of arc, angle of arc and height of the triangle, respectively. The area of arc is calculated using relation:

$$A_{arc} = \frac{1}{2} R_{arc}^2 \theta_{arc} \quad (11)$$

TABLE 2. LHS Design Samples

X_1 (mm)	X_2 (mm)	Voltage (V)	Cogging Torque (Nm)
1.857	49.143	19.68	1.33
1.4	47	19.34	1.38
2.086	49.857	19.66	1.28
1.8	51.286	18.84	1.33
1.629	48.429	18.44	1.34
1.514	45.571	19.08	1.27
1.8	47	19.06	1.28
2.029	47.714	19.24	1.25
1.914	44.857	18.52	1.30
1.743	42	19.62	1.30
1.971	42.714	19.06	1.22
1.457	43.429	19.3	1.26
2.143	46.286	18.82	1.27
1.686	44.143	19.54	1.23
1.852	46.791	19.15	1.24

Whilst the area of the proposed shape is calculated as:

$$A_{arc} = \frac{1}{2}R_{arc}^2\theta_{arc} + \frac{1}{2}lb \tag{12}$$

The total volume of the arc shaped magnet is the product of total area and height, mathematically:

$$V_t = A_{arc}H_o \tag{13}$$

The selected variables optimized in the range given below:

- $42 < X_1 < 52$ mm
- $1.4 < X_2 < 2.2$ mm

B. PROCESS OF OPTIMIZATION

A flow chart of the optimization process based on the selected variables is depicted in Figure 7 Initially, design variables and objective function are chosen. Latin hyper cube sampling (LHS) is used for designing the samples by space filling by using equal samples points in a given parameter space. LHS is then used to calculate the average, change, and function distribution of the output. In addition, LHS also confirms that all input parameters are within the range. MATLAB Model Based Calibration Tool is used to save time in determining the optimum response. The total number of design samples chosen are 15, as evident from Table 2, whereas equal volume of the magnets is selected in all samples.

Then, three-dimensional (3D) Finite Element Analysis (FEA) is used for the performance analysis because of 3D

- **Objective Function:**
Minimization of Cogging Torque
- **Design Variables:**
 $42\text{mm} < X_1 < 52\text{mm}$
 $1.4\text{mm} < X_2 < 2.2\text{mm}$
- **Constraints:**
Cogging Torque $< 1.0\text{Nm}$
(peak to peak)

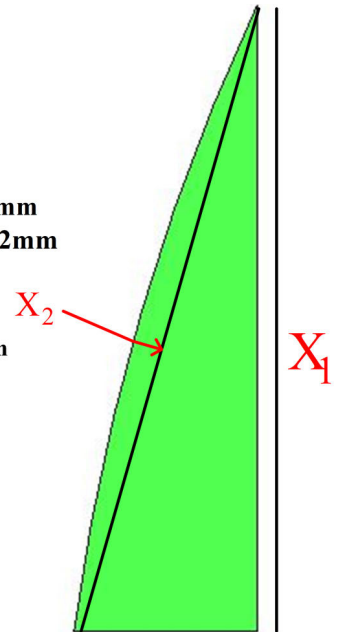


FIGURE 6. Design variables used for the optimization of the proposed model.

electromagnetic behavior of the proposed machine topology. The FEA is preferred over analytical techniques (Equivalent Circuit, Fourier Series) because it considers the process of saturation [25].

TABLE 3. Result Comparison

Parameters	Conventional Model	Proposed Model	Optimized Model
Back EMF	22V	19.5V	23.5V
Cogging Torque (peak to peak)	1.7Nm	0.65Nm	0.61Nm
Rated Torque	61Nm	57.2Nm	61.7Nm

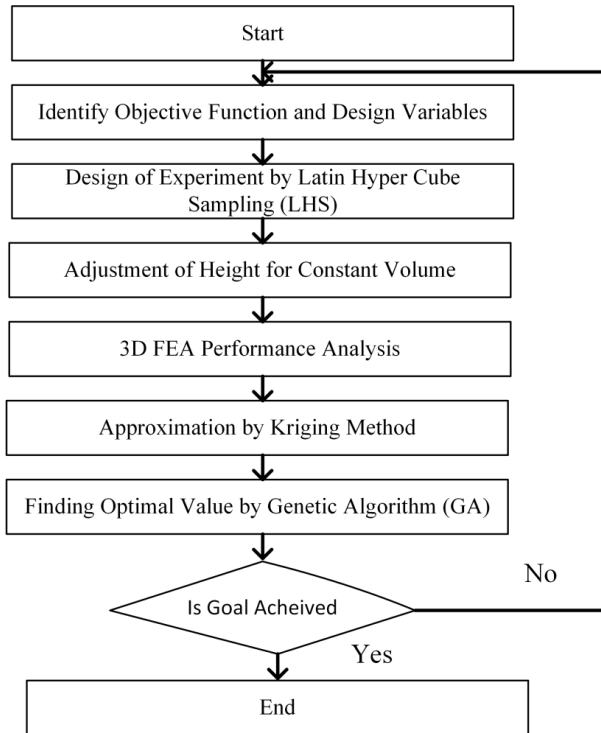


FIGURE 7. Optimization process.

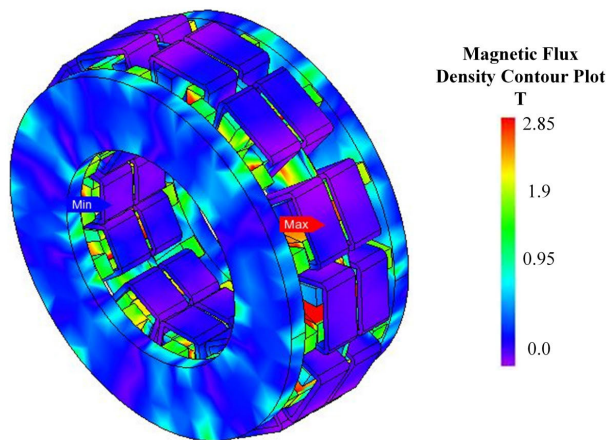


FIGURE 8. Flux density distribution of the optimized model.

The Kriging method is employed in the approximation of the objective function.

The genetic algorithm (GA) is used to find the optimal values of the design variables and the objective function. The optimal values of X_1 and X_2 obtained from the GA are

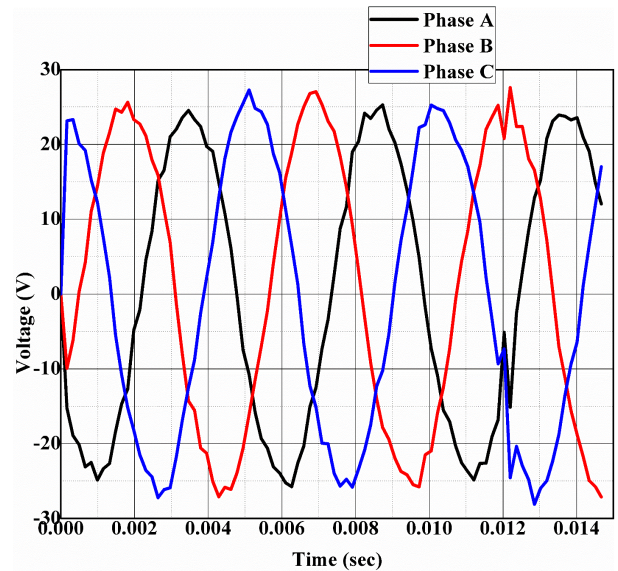


FIGURE 9. Back EMF of the optimized model.

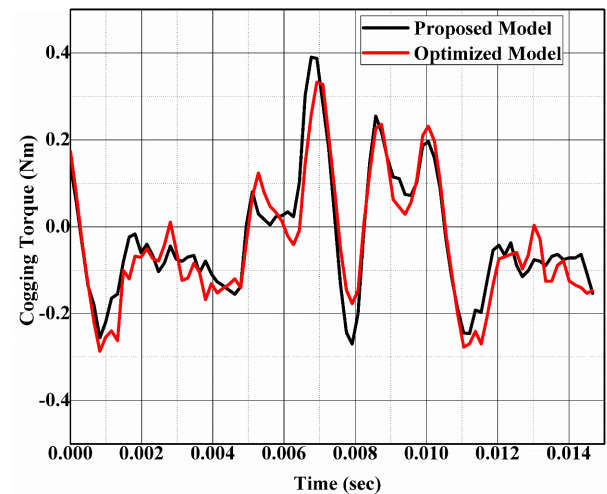


FIGURE 10. Cogging torque comparison of the proposed and optimized models.

1.79 mm and 46.41 mm, respectively. Finally, a 3D FEA is performed to verify the optimal results.

C. OPTIMIZATION RESULTS

Figure 8 shows the flux density distribution of the optimized model. The maximum flux density distribution is 2.85 T in the optimized model. Due to increase in the flux density, back emf increases, as depicted in Figure 9.

Figure 10 shows a comparison between the cogging torque of the proposed and the optimized model. The results show that the cogging torque of the optimized model is decreased as compared to the proposed model. Overall, 6.15% reduction in the cogging torque is observed. However, the rated torque increases to 61.7 Nm in optimized model. The results comparison is drawn in Table 3.

V. CONCLUSION

A model of axial field FSPMM with arc shaped triangular magnet is proposed in this research. The analysis showed that the cogging torque is significantly decreased in the proposed model but at the cost of slight decrease in the rated torque. However, torque ripples are considerably reduced in the proposed model. In particular, 61.8% decrease in peak-to-peak value of the cogging torque as compared to conventional model is achieved. Further, the optimization of the proposed model is performed to improve the proposed machine performance using equal volume of the arc shaped magnets. The optimization demonstrated that 6.15 % reduction in the cogging torque can be further obtained as compared to the proposed model. Overall, the optimized model shows better results as compared to both the conventional and the proposed axial field FSPMMs.

REFERENCES

- [1] J. Yan, H. Lin, and Y. Feng, "Flux switching transverse flux permanent magnet wind generator," (in Chinese), *Proc. Chin. Soc. Elect. Eng.*, vol. 30, no. 21, pp. 67–72, 2010.
- [2] Y. J. Bao, K. W. E. Cheng, X. D. Xue, J. Chan, Z. Zhang, and J. K. Lin, "Research on a novel switched reluctance generator for wind power generation," in *Proc. 4th Int. Conf. Power Electron. Syst. Appl.*, Hong Kong, Jun. 2011, pp. 1–6.
- [3] T. F. Chan and L. L. Lai, "An axial flux permanent magnet synchronous generator for direct-coupled wind-turbine system," *IEEE Trans. Energy Convers.*, vol. 22, no. 1, pp. 86–94, Jan. 2007.
- [4] Y. Chen, P. Pillay, and A. Khan, "PM wind generator topologies," *IEEE Trans. Ind. Appl.*, vol. 41, no. 6, pp. 1619–1626, Nov. 2005.
- [5] F. Caricchi, F. Crescimbeni, and O. Honrati, "Modular axial-flux permanent-magnet motor for ship propulsion drives," *IEEE Trans. Energy Convers.*, vol. 14, no. 3, pp. 673–679, Sep. 1999.
- [6] A. Parviainen, J. Pyrhonen, and P. Konthanen, "Axial flux permanent magnet wind generator with concentrated winding for small wind power applications," in *Proc. Int. Conf. Electric Mach. Drives*, San Antonio, TX, USA, 2005, pp. 1187–1191.
- [7] E. Hoang, A. H. Ben-Ahmed, and J. Lucidarme, "Switching flux permanent magnet polyphased synchronous machines," in *Proc. 7th Eur. Conf. Power Electron. Appl.*, vol. 3, 1997, pp. 303–303.
- [8] W. Hua, M. Cheng, Z. Q. Zhu, and D. Howe, "Study on static characteristics of novel flux-switching doubly salient PM machine," (in Chinese), *Proc. Chin. Soc. Elect. Eng.*, vol. 26, no. 13, pp. 129–134, 2006.
- [9] Z. Q. Zhu, Y. Pang, D. Howe, S. Iwasaki, R. Deodhar, and A. Pride, "Analysis of electromagnetic performance of flux-switching permanent-magnet machines by nonlinear adaptive lumped parameter magnetic circuit model," *IEEE Trans. Magn.*, vol. 41, no. 11, pp. 4277–4287, Nov. 2005.
- [10] J. T. Chen, Z. Q. Zhu, and D. Howe, "Stator and rotor pole combinations for multi-tooth flux-switching permanent-magnet brushless AC machines," *IEEE Trans. Magn.*, vol. 44, no. 12, pp. 4659–4667, Dec. 2008.
- [11] J. T. Chen, Z. Q. Zhu, S. Iwasaki, and R. Deodhar, "A novel E-core flux switching PM brushless AC machine," *IEEE Trans. Ind. Appl.*, vol. 47, no. 3, pp. 1273–1282, Mar. 2011.
- [12] A. S. Thomas, Z. Q. Zhu, R. L. Owen, G. W. Jewell, and D. Howe, "Multi-phase flux-switching permanent-magnet brushless machine for aerospace application," *IEEE Trans. Ind. Appl.*, vol. 45, no. 6, pp. 1971–1981, Jun. 2009.
- [13] A. Zulu, B. C. Mecrow, and M. Armstrong, "Permanent-magnet flux-switching synchronous motor employing a segmental rotor," *IEEE Trans. Ind. Appl.*, vol. 48, no. 6, pp. 2259–2267, Nov./Dec. 2012.
- [14] D. G. Dorrell, M.-F. Hsieh, and A. M. Knight, "Alternative rotor designs for high performance brushless permanent magnet machines for hybrid electric vehicles," *IEEE Trans. Magn.*, vol. 48, no. 2, pp. 835–838, Feb. 2012.
- [15] W. Cao, B. C. Mecrow, G. J. Atkinson, J. W. Bennett, and D. J. Atkinson, "Overview of electric motor technologies used for more electric aircraft (MEA)," *IEEE Trans. Ind. Electron.*, vol. 59, no. 9, pp. 3523–3531, Aug. 2011.
- [16] M. Cheng, W. Hua, J. Jhang, and W. Zhao, "Overview of stator permanent magnet brushless machines," *IEEE Trans. Ind. Electron.*, vol. 58, no. 11, pp. 5087–5101, Nov. 2011.
- [17] X. Xue, W. Zhao, J. Zhu, G. Liu, X. Zhu, and M. Cheng, "Design of five phase modular flux switching permanent magnet machines for high reliability applications," *IEEE Trans. Magn.*, vol. 49, no. 7, pp. 3941–3944, Jul. 2013.
- [18] W. Min, J. T. Chen, Z. Q. Zhu, Y. Zhu, M. Zhang, and G. H. Duan, "Optimization and comparison of novel E-core and C-core linear switched flux PM machines," *IEEE Trans. Mag.*, vol. 47, no. 8, pp. 2134–2141, Aug. 2011.
- [19] M. J. Jin, C. F. Wang, J. X. Shen, and B. Xia, "A modular permanent magnet flux switching linear machine with fault tolerant capability," *IEEE Trans. Magn.*, vol. 45, no. 8, pp. 3179–3186, Aug. 2009.
- [20] L. Hao, M. Lin, X. Zhao, X. Fu, Z. Q. Zhu, and P. Jin, "Static characteristics analysis and experimental study of a novel axial field flux switching permanent magnet generator," *IEEE Trans. Magn.*, vol. 48, no. 11, pp. 4212–4215, Nov. 2012.
- [21] R. L. Owen, Z. Q. Zhu, and G. W. Jewell, "Hybrid-excited flux-switching permanent-magnet machines with iron flux bridges," *IEEE Trans. Magn.*, vol. 46, no. 6, pp. 1726–1729, Jun. 2010.
- [22] W. Fei, P. C. K. Luk, and J. Shen, "Torque analysis of permanent-magnet flux switching machines with rotor step skewing," *IEEE Trans. Magn.*, vol. 48, no. 10, pp. 2664–2673, Oct. 2012.
- [23] Y. Wang, M. Chen, T. W. Ching, and K. T. Chau, "Design and analysis of a new HTS axial-field flux-switching machine," *IEEE Trans. Appl. Supercond.*, vol. 25, no. 3, pp. 1–5, Nov. 2014.
- [24] L. Hao, M. Lin, W. Li, H. Luo, X. Fu, and P. Jin, "Novel dual rotor axial field flux switching permanent magnet machine," *IEEE Trans. Magn.*, vol. 48, no. 11, pp. 4232–4235, Nov. 2012.
- [25] M. Lin, L. Hao, X. Li, X. Zhao, and Z. Q. Zhu, "A novel axial field flux-switching permanent magnet wind power generator," *IEEE Trans. Magn.*, vol. 47, no. 10, pp. 4457–4460, Oct. 2011.
- [26] W. Zhao, T. A. Lipo, and B. I. Kwon, "A novel dual-rotor, axial field, fault-tolerant flux-switching permanent magnet machine with high-torque performance," *IEEE Trans. Magn.*, vol. 51, no. 11, pp. 707–715, Jun. 2015.



MIRZA AAKIF BAIG received the B.S. and M.S. degrees in electrical engineering from COMSATS University Islamabad, Islamabad, Pakistan, in 2017 and 2020, respectively. He is currently a Lecturer with Arid University Rawalpindi, Pakistan. His research interests include the design, analysis, modeling, and control of electric machines.



JUNAID IKRAM received the B.E. degree in electrical engineering from the University of Engineering and Technology Lahore, Pakistan, in 2005, the M.S. degree from Hanyang University, South Korea, in 2009, and the Ph.D. degree in electrical engineering from COMSATS University Islamabad, Pakistan, in 2017. He is currently a Senior Engineer with COMSATS University Islamabad. His research interests include design, analysis and optimization of axial flux machines,

Vernier machines, wound rotor synchronous machine, hybrid flux switching machines, and the modeling of the machine losses.



ADNAN IFTIKHAR (Member, IEEE) received the B.S. degree in electrical engineering from COMSATS University Islamabad (CUI), Pakistan, in 2008, the M.S. degree in personal mobile and satellite communication from the University of Bradford, U.K., in 2010, and the Ph.D. degree in electrical and computer engineering from North Dakota State University (NDSU), USA, in 2016.

He is currently an Assistant Professor with the Department of Electrical and Computer Engineering, CUI. He has authored or coauthored 50 journals and conference publications. His current research interests include applied electromagnetic, reconfigurable antennas, leaky wave antennas, phased array antennas, and energy harvesting for low power devices.



NASRULLAH KHAN (Senior Member, IEEE) received the B.Sc. degree in electrical engineering degree from UET Lahore, in 1984, the M.Sc. degree from Reading University, U.K., in 1988, and the Ph.D. degree from Essex University, U.K., in 1992. He has 21 years teaching and research, and 12 years practical field experience. He has done several research projects in COMSATS and abroad. He has 34 years local and foreign teaching, research, and field experience.



SYED SABIR HUSSAIN BUKHARI (Member, IEEE) received the B.E. degree in electrical engineering from the Mehran University of Engineering and Technology, Jamshoro, Pakistan, in 2009, and the Ph.D. degree from the Department of Electronic Systems Engineering, Hanyang University, South Korea, in 2017. In December 2016, he joined an Assistant Professor Sukkur IBA University. He is currently a Research Professor with Chung-Ang University, Seoul, South Korea under

Korean Research Fellowship (KRF) Program. His current research interests include electric machine design, power quality, and drive controls.



JONG-SUK RO received the B.S. degree in mechanical engineering from Han-Yang University, Seoul, South Korea, in 2001, and the Ph.D. degree in electrical engineering from Seoul National University (SNU), Seoul, South Korea, in 2008.

From 2008 to 2012, he conducted research at the Research and Development center of Samsung Electronics as a Senior Engineer. From 2012 to 2013, he was with the Brain Korea 21 Information Technology, SNU, as a Postdoctoral Fellow. In 2013, he conducted research with the Electrical Energy Conversion System Research Division, Korea Electrical Engineering & Science Research Institute as a Researcher. From 2013 to 2016, he was with the Brain Korea 21 Plus, SNU, as a BK Assistant Professor. In 2014, he was with the University of Bath, Bath, U.K. He is currently an Associate Professor of the School of Electrical and Electronics Engineering, Chung-Ang University, Seoul, South Korea. His research interests include the analysis and optimal design of next-generation electrical machines using smart materials such as electromagnet, piezoelectric, and magnetic shape memory alloy.

...